P-ISSN 2586-9000
E-ISSN 2586-9027
Homepage : *https://tci-thaijo.org/index.php/SciTechAsia* **Science & Technology Asia**
Vol.24 No.1 January - March 2019 **Page [1-13]**
Original research article

Heat Transfer Characteristics of Nanofluid Due to a Permeable Rotating Disk with Slip Effect and Thermophoresis

Asiya Khatun[1], Mohammad Mahabubur Rahman[2,*] and Shariful Alam[3]

[1]*Department of Mathematics, Jagannath University, Dhaka-1100, Bangladesh.*
[2]*Department of Electrical and Electronic Engineering, Sonargaon University, Dhaka-1215, Bangladesh.*
[3]*Department of Mathematics, Jagannath University, Dhaka-1100, Bangladesh.*

Received 22 July 2018; Received in revised form 23 October 2018
Accepted 23 October 2018; Available online 8 February 2019

ABSTRACT

The main purpose of the current study is to represent numerical simulations for magneto-nanofluid slip flow and heat transfer over a permeable rotating disk in the presence of thermophoresis and Brownian motion. To carry out the experiment, the governing nonlinear partial differential equations are converted into nonlinear ordinary differential equations by using similarity analysis and the solutions are computed through the algebra software MATLAB. The obtained results are consistent with previously available studies to a particular extent. The natures of the involved interesting parameters on the temperature and concentration are drawn graphically. The present study further computes and examines the local Nusselt Number. The emerged results may be useful for environmental, industrial and engineering phenomena.

Keywords: Nanofluids; Heat transfer; MHD; Brownian motion; Rotating disk.

1. Introduction

Nanofluids are a contemporary branch of nanotechnology, based on heat transfer fluids, gained by dispersing and suspending nanoparticles with a prototypical size of 10 nm. The properties of nanofluids have motivated students, scientists, and engineers around the world to undertake the challenge of exploring the possibilities of these captivating fluids. The word nanofluids was first coined by Choi [1] to describe the new class of fluids. In nanofluids, various types of liquids, for example, water, ethylene- or tri-ethylene-glycols, and other coolants; oil and other lubricants; bio-fluids, polymer solutions and other common fluids have been used as host liquids. On the other hand, nanoparticles

*Corresponding author: mrahman78793@gmail.com **doi:** 10.14456/scitechasia.2019.1

used in nanofluids include various materials, such as oxide ceramics (Al_2O_3, CuO), carbide ceramics (SiC, TiC), metals (Cu, Ag, Au, Fe), nitride ceramic (AlN, SiN), semiconductors (TiO_2, SiC), etc. The combinations of nanoparticles and base fluids may produce many heterogeneous nanofluids. The thermal conductivity of the base fluids plays a significant role on the heat transfer coefficient between the heat transfer medium and the heat transfer surface. Therefore, the effective thermal conductivity of nanofluids is expected to enhance heat transfer compared with conventional heat transfer liquids (Masuda et al. [2]). This phenomenon indicates the probability of using nanofluids in advanced nuclear systems (Buongiorno and Hu [3]). The improved thermal performance of nanofluids is beneficial for wide-ranging applications including solar water heating, delivery of drugs and radiation in patients, cooling of microelectronics, improving heat transfer efficiency of refrigerators and chillers, cooling of machine equipment, cooling of transformer oil, nuclear reactor cooling, and optimal absorption of solar energy and in improving transportation. Some comprehensive review studies about the potential applications of nanofluids are presented by Kakac´ and Pramuanjaroenkij [4], Wong and Leon [5], Saidur et al. [6] and Wen et al. [7]. Nanoparticles have unique chemical and physical properties (Oztop and Abu-Nada [8]) and have better thermal conductivity and convective heat transfer coefficient compared to the base fluid only. Choi [1] figured that the addition of a small amount, less than 1% by volume, of nanoparticles to conventional heat transfer liquids increased the thermal conductivity of the fluid up to approximately two times. It can be mentioned the valuable recently published book by Das et al. [9] entitled Nanofluids: Science and Technology. Buongiorno and Hu [3] noticed that several authors have suggested that convective heat transfer enhancement could be due to the dispersion of the suspended nanoparticles, but they argue that this effect is too small to explain the observed enhancement. They also conclude that turbulence is not affected by the presence of the nanoparticles so this cannot be explained by the observed enhancement. In another study, Buongiorno [10] has indicated that the absolute velocity of nanoparticles can be viewed as the sum of the base fluid velocity and a relative velocity (that he calls the slip velocity). In his paper, he assumed the seven slip mechanisms: inertia, thermophoresis, diffusiophoresis, Brownian diffusion, fluid drainage, Magnus effect, and gravity settling. By considering all the time scales of these processes, he concluded that for laminar flow (also in the viscous sub-layer of the turbulent flow) thermophoresis and Brownian diffusion are an important mechanism, while in the turbulent region the nanoparticles are carried by turbulent eddies without slip and the diffusion mechanisms above are negligible there. Based on these assumptions, he also derived the continuity equation for nanofluids and nanoparticle volume fraction. The steady boundary-layer flow of a nanofluid past a moving semi-infinite flat plate in a uniform free stream has been examined by Bachok et al. [11]. Rajput et al. [12] studied the boundary layer flow of electrically conducting, viscous incompressible nanofluids over a moving surface in the presence of a uniform magnetic field. The 3-D viscous flow induced by a uniformly rotating disk containing constant angular velocity was first figured out by Von Karman [13]. These type of flow problems have significance in enormous applications such as the dynamics of hurricanes and tornadoes, rotor–stator systems in turbines, food processing, geothermal extraction, chemical mixing chambers, designing of nuclear reactors, power generators,

computer storage devices, oil recovery process, and many others. Suction/injection effects on the swirling flow due to a permeable rotating disk were studied by Nanda [14]. Heat transfer characteristics for laminar flow over a rotating disk were investigated by Millsaps and Pohlhausen [15]. Batchelor [16] presented one parameter family of solutions for flow over a disk subjected to uniform rotation, and the fluid far from the disk was assumed to rotate like a rigid body. A monograph concerning an excellent review about the rotating flow problems was published by Owen and Rogers [17]. Unsteady revolving flow near a permeable surface was discussed by Attia [18] using the finite difference approach. He examined heat transfer characteristics on steady revolving flow induced via a permeable heated disk. Bachok et al. [19] compared two different nanofluid models for laminar flow adjacent to a stationary rotating disk. The heat transfer mechanism in swirling flow adjacent to a rotating disk with partial slip was examined by Turkyilmazoglu and Senel [20]. Recently, Shafique et al. [21] studied the onset of activation energy on Maxwell fluid flow in a rotating frame utilizing a numerical approach. Mushtaq et al. [22] explored the nanofluid flow past an exponentially stretchable surface using the Maxwell model of thermal conductivity. Rida and Mustafa [23] compared thermal conductivity models for nanofluid convective transport over an exponentially deforming surface. Thus, the purpose of the present study is to explore the unsteady magneto-nanofluid flow due to a porous rotating disk. The thermophoretic effect and Brownian motion phenomena take place due to consideration of nanoparticles. We also employed the velocity slip condition. In most of the cases, the velocity slip between moving surface and fluid may occur when the liquid is particulate such as suspensions, emulsions, rarefied gas, etc. Under such conditions, the suitable boundary condition is developed by Navier Stoke's equation and is known as the slip condition. The governing mathematical problem along with the boundary condition is computed numerically by bvp4c technique. The obtained numerical results are plotted and discussed for different values of parameters. Finally, the heat transfer rate in terms of the local Nusselt number is calculated for different values of dimensionless parameters and shown in tabular form.

2. Mathematical Modeling

In a non-rotating cylindrical polar frame of reference, where z is the vertical axis in the cylindrical coordinates system with r and φ as the radial and tangential axes respectively, let us consider a disk which rotates with constant angular velocity about the z axis. The disk is placed at $z = 0$ and a viscous incompressible Newtonian and electrically conducting nanofluid occupies the region $z > 0$. The flow configurations and geometrical coordinates are shown in Fig. 1.

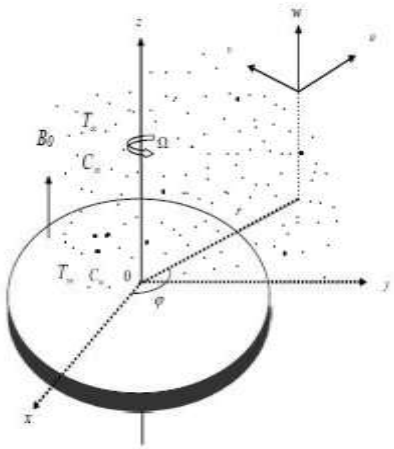

Fig. 1. Physical configuration and coordinate system.

The components of the flow velocity are in the direction of increasing (r, φ, z), respectively. An external uniform magnetic field is applied perpendicular to the surface (i.e. the z direction) of the disk and has a

constant magnetic flux density (or, applied magnetic field) B_0 everywhere in the fluid. The surface of the rotating disk is maintained at a uniform temperature T_w and far away from the wall, the free stream temperature is T_∞ ($T_w > T_\infty$). At $t < 0$ the fluid is at rest and at constant temperature and concentration and the disk does not rotate. At $t = 0$ the disk is instantaneously put into a motion (impulsively accelerated) at constant angular velocity. Because of this, the flow is actually transient during a very small time interval before reaching the well-known steady-state. The effects of thermophoresis and Brownian motion are being taken into account to help in the understanding of the mass deposition variation on the surface. In the present study, we consider the nanofluid as a two-component mixture (i.e. base fluid plus nanoparticle) with the assumptions (i) incompressible flow, (ii) no chemical reaction, (iii) dilute mixture, (iv) negligible viscous dissipation, (v) nanoparticles and the base fluid locally in thermal equilibrium. Under the above-mentioned assumptions, the governing equations for the present problem can be written as (see also Buongiorno [10] and Hayat et al. [24]).

$$\frac{\partial u}{\partial r}+\frac{u}{r}+\frac{\partial w}{\partial z}=0 \qquad (1)$$

$$\frac{\partial u}{\partial t}+u\frac{\partial u}{\partial r}-\frac{v^2}{r}+w\frac{\partial u}{\partial z}=-\frac{1}{\rho}\frac{\partial \rho}{\partial r}+\upsilon\left(\frac{\partial^2 u}{\partial r^2}+\frac{1}{r}\frac{\partial u}{\partial r}-\frac{u}{r^2}+\frac{\partial^2 u}{\partial z^2}\right)-\frac{\sigma B^2{}_0}{\rho}u \qquad (2)$$

$$\frac{\partial v}{\partial t}+u\frac{\partial v}{\partial r}+\frac{uv}{r}+w\frac{\partial v}{\partial z}=\upsilon\left(\frac{\partial^2 v}{\partial r^2}+\frac{1}{r}\frac{\partial v}{\partial r}-\frac{v}{r^2}+\frac{\partial^2 v}{\partial z^2}\right)-\frac{\sigma B^2{}_0}{\rho}v \qquad (3)$$

$$\frac{\partial w}{\partial t}+u\frac{\partial w}{\partial r}+w\frac{\partial u}{\partial z}=-\frac{1}{\rho}\frac{\partial \rho}{\partial z}+\upsilon\left(\frac{\partial^2 w}{\partial r^2}+\frac{1}{r}\frac{\partial w}{\partial r}+\frac{\partial^2 w}{\partial z^2}\right) \qquad (4)$$

$$\frac{\partial T}{\partial t}+u\frac{\partial T}{\partial r}+w\frac{\partial T}{\partial z}=\alpha\left(\frac{\partial^2 T}{\partial r^2}+\frac{1}{r}\frac{\partial T}{\partial r}+\frac{\partial^2 T}{\partial z^2}\right)+\frac{(\rho c_\rho)_p}{(\rho c_\rho)_f}[D_B(\frac{\partial C}{\partial z}\frac{\partial T}{\partial z}+\frac{\partial C}{\partial r}\frac{\partial T}{\partial r})+\frac{D_T}{T_\infty}((\frac{\partial T}{\partial r})^2+(\frac{\partial T}{\partial z})^2)] \qquad (5)$$

$$\frac{\partial C}{\partial t}+u\frac{\partial C}{\partial r}+w\frac{\partial C}{\partial z}=D_B\left(\frac{\partial^2 C}{\partial r^2}+\frac{1}{r}\frac{\partial C}{\partial r}+\frac{\partial^2 C}{\partial z^2}\right)+\frac{D_T}{T_\infty}\left(\frac{\partial^2 T}{\partial r^2}+\frac{1}{r}\frac{\partial T}{\partial r}+\frac{\partial^2 T}{\partial z^2}\right) \qquad (6)$$

where $\upsilon = (\mu/\rho)$ is the kinematic viscosity, μ is the dynamic viscosity, ρ is the density of base fluid, σ is the electrical conductivity, $\alpha = \dfrac{k}{(\rho c_p)_f}$ the thermal diffusivity of fluid, k is the thermal conductivity of fluid, $(\rho c_p)_f$ is the heat capacity of fluid, $(\rho c_p)_p$ is the effective heat capacity of nanoparticles, D_B is the Brownian diffusion coefficient and D_T is the thermophoretic diffusion coefficient. If mean free path of the fluid particles is comparable to the characteristics dimensions of the flow field domain, the assumption of continuum media is no longer valid and, as a consequence, Navier–Stokes equations break down. In the range of

$0.1 < Kn < 10$ the higher order continuum equation should be used. For the range of $0.001 < Kn < 0.10$, the no-slip boundary condition cannot be used and should be replaced with $U_t = \lambda^*(\frac{2-\zeta}{\zeta})\frac{\partial u}{\partial z}$ where U_t is the target velocity and ζ is the target momentum accommodation coefficient and λ^* is the mean free path. For $Kn < 0.001$, the no-slip boundary condition is valid; therefore, the velocity at the surface is equal to zero. In this study, the slip and the no-slip regimes of the Knudsen number that lies in the range $0 < Kn < 0.1$ are considered.

2.1 Boundary Conditions

(i) On the surface of the disk ($z = 0$)

$$u = U_t,\ v = \Omega r + U_t,$$
$$w = w_{S,}\ p = 0,\quad T = T_w,$$
$$C = C_w \ at\ z \to 0 \qquad (7)$$

(ii) Matching with the quiescent free stream $(z \to \infty)$

$$u = 0, v = 0,\ \ p \to p_\infty,$$
$$T \to T_\infty,\ C \to C_\infty$$
$$as\ z \to \infty \qquad (8)$$

3. Dimensionless Governing Equation

To obtain the similarity solutions of the governing equations (1)-(6) along with the boundary conditions (7)-(8) we introduce the following similarity transformations:

$$\eta = \frac{z}{\delta},\ u = \Omega r F(\eta),\ \ v = \Omega r G(\eta),$$
$$w = \frac{\upsilon}{\delta}\ H(\eta),\ \ p = -\rho\upsilon\Omega P(\eta), \qquad (9)$$
$$\theta(\eta) = \frac{T - T_\infty}{T_w - T_\infty},\ \ \phi(\eta) = \frac{C - C_\infty}{C_w - C_\infty},$$

where δ is a scale factor and is a function of time as $\delta = \delta(t)$.

Substituting (9) into equations (1) - (6), we obtain the following differential equations:

$$H' + 2RF = 0 \qquad (10)$$
$$F'' - HF' - R(F^2 - G^2) + \lambda\eta F' - MF = 0 \qquad (11)$$
$$G'' - HG' - 2RFG + \lambda\eta G' - MG = 0 \qquad (12)$$
$$H'' - HH' + RP' + \lambda\eta H' = 0 \qquad (13)$$
$$\theta'' - \Pr H\theta' + \Pr\lambda\eta\theta' + Nb\theta'\phi'\Pr + Nt\theta'^2\Pr = 0 \qquad (14)$$
$$\phi'' + Le\lambda\eta\theta' - LeH\phi' + \frac{Nt}{Nb}\theta'' = 0 \qquad (15)$$

With transformed boundary condition as

$$F = \epsilon F', G = 1 + \epsilon G', H = w_w, P = o,$$
$$\theta = 1, \phi = 1\ \ at\ \ \eta = 0 \qquad (16)$$
$$F = 0, G = 0, \theta = 0, \phi = 0\ as\ \eta \to \infty \qquad (17)$$

where $\epsilon = \frac{\lambda}{\delta}\frac{2-\varsigma}{\varsigma}$ is the slip parameter and $w_w = \frac{w_s\delta}{\upsilon}$ represents a uniform suction($w_w < 0$) or injection ($w_w > 0$) at the surface, $R = \frac{\Omega\delta^2}{\upsilon}$ is the rotational parameter, $\lambda = \frac{\delta}{\upsilon}\frac{d\delta}{dt}$ is the unsteadiness parameter, $\Pr = \frac{\upsilon}{\alpha}$ is the Prandtl number, $Nt = \frac{\tau D_T \Delta T}{T_\infty \upsilon}$ is the thermophoresis

parameter, $Nb = \dfrac{\tau D_B \Delta C}{\upsilon}$ is the Brownian diffusion parameter, $Le = \dfrac{\upsilon}{D_B}$ is the Lewis number and $M = \dfrac{\alpha B^2{}_0 \delta^2}{\rho \upsilon}$ is the magnetic field parameter.

4. Rate of heat transfer

The rate of heat transfer from the disk surface to the nanofluid is computed by the application of Fourier's law as given below

$$q_w = -k \frac{\partial T}{\partial z}_{z=0} = k \frac{T_\infty - T_w}{\delta} \theta'(0)$$

Hence the Nusselt number is obtained as

$$Nu = \frac{\delta q_w}{k(T_\infty - T_w)} = -\theta'(0) \ .$$

5. Code Validation

When λ = 0 (i.e. for steady case), $R = 1, M = 0, w_w = 0, \epsilon = 0$ and in the absence of heat and mass transfer, the present problem shows the excellent agreement with the study of White [25] . To assess the accuracy of the present code, we have calculated the values of $F, G, and\ H$ for different values of η in the absence of heat and mass transfer. Table 1 presents a comparison of the data obtained in the present work and those obtained by White [25]. It is vividly observed that very good consistencies exist between the results. This leads to confidence in the present numerical method.

6. Numerical Solutions

The set of (10)-(15) are highly nonlinear and coupled and therefore cannot be solved analytically. We canceled (13) from the system as it can be used for calculating pressure once H is known from the rest of the equations. The transformed governing (10)-(12) and (14)-15) with boundary conditions (16)-(17) are solved numerically by using the algebra software MATLAB. The software is well tested and has been successfully used to study a wide variety of nonlinear heat, mass, and fluid flow problems.

7. Numerical results and discussion

For the purpose of discussing the results, the numerical calculations are presented graphically for non-dimensional temperature and concentration profiles as a function of η whereas the rates of heat transfer are shown in tabular form. Because of the lack of experimental data, the choice of the parameters is dictated by the values chosen by previous investigators. In the present investigation, we considered water-based nanofluids (containing Cu, Al_2O_3, TiO_3, etc. nanoparticles). The value of $\Pr = 6.2$ (at the room temperature) is assumed. From Fig. 2(a), it can be predicted that the temperature of the fluid within the boundary layer increases with the increase of the magnetic field parameter. Larger values of magnetic field parameter correspond to a stronger thermal diffusivity. Such stronger thermal diffusivity creates the increment of temperature profile.

It can be observed from Fig. 2(b) as magnetic field parameter enlarges the concentration profile increases**.** The values of magnetic field parameter are related to the concentration profile proportionally. So, higher values of magnetic field parameter imply the increment of the concentration profile.

It can be indicated from Fig. 3(a) that the temperature profile in the fluid flow is suppressed according to the increased values of the unsteadiness parameter because it prevents the profile of temperature. On the other hand, the concentration profile is reduced for the larger values of the unsteadiness parameter because it is oppositely associated with concentration which is shown in Fig. 3(b).

The effect of R on the temperature profile is depicted in Fig. 4(a). The increased values of R lead to the thermal boundary layers decrease because it retards the temperature profile.

However, the concentration profile within the fluid flow decreases with the increase of the rotational parameter which is pictured in Fig. 4(b). The increased values of R imply that lower concentration and it also causes less diffusive flux. Consequently, larger values of R insinuate a lower diffusion rate.

The influence of ϵ on temperature field θ is sketched in Fig. 5(a). This figure shows that slip causes an increment in the temperature field.

The concentration of the particles within the boundary layer increases with the increase of the slip parameter shown from Fig. 5(b). Quite interestingly, we have found that the effects of the slip parameter on concentration are quite similar to the effect of the slip parameter on temperature. Conclusively, one can control the thermal and concentration boundary layer up to the desired values by adjusting the slip parameters.

The impact of Brownian motion parameter Nb on the temperature profile is depicted in Fig. 6(a). It is suggested that the downward trend occurs in the temperature profile when the larger values of Brownian motion parameter are accounted for. Such larger Brownian motion parameters have higher a Brownian diffusion coefficient and smaller viscous force which holds back the thermal boundary layer.

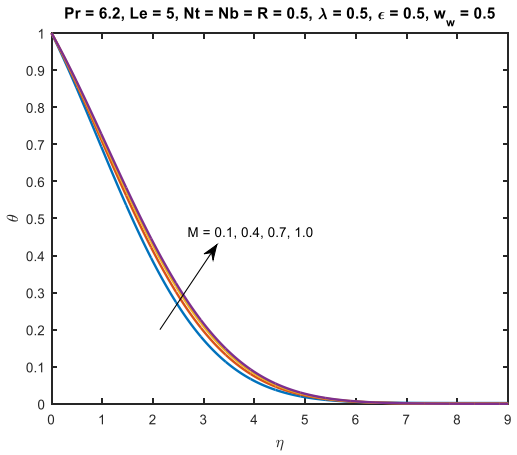

Fig. 2(a). Temperature profile for various values of M.

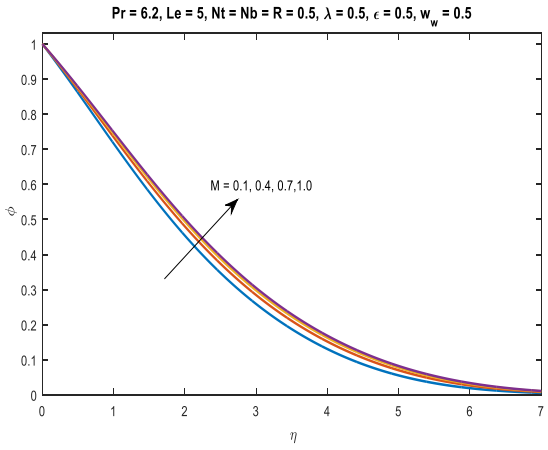

Fig. 2(b). Concentration profile for various values of M.

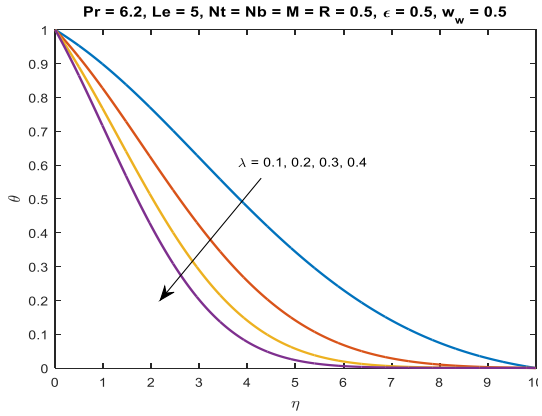

Fig. 3(a). Temperature profile for various values of λ.

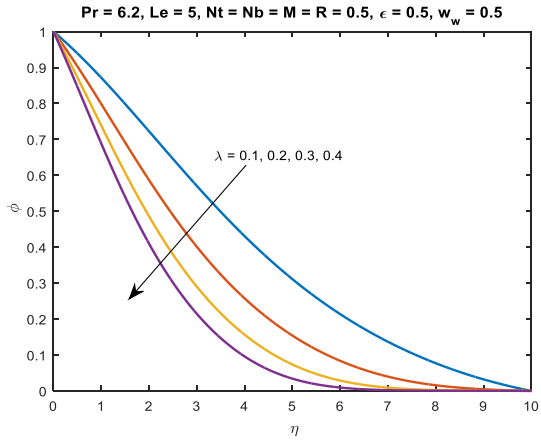

Fig. 3(b). Concentration profile for various values of λ .

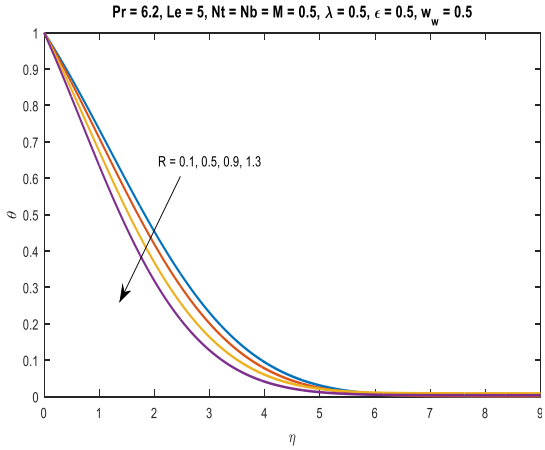

Fig. 4(a). Temperature profile for various values of R .

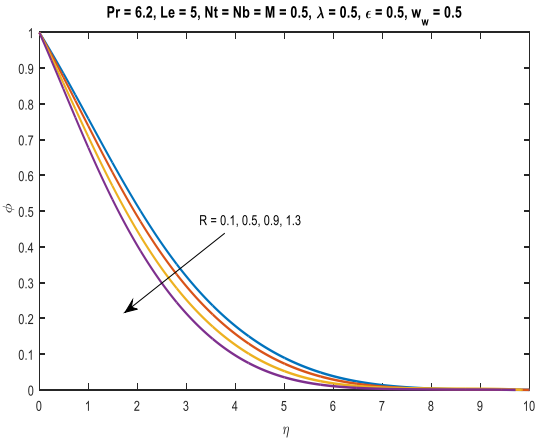

Fig. 4(b). Concentration profile for various values of R .

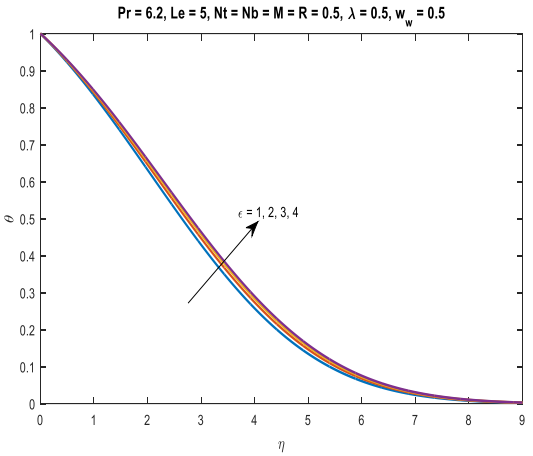

Fig. 5(a). Temperature profile for various values of ϵ .

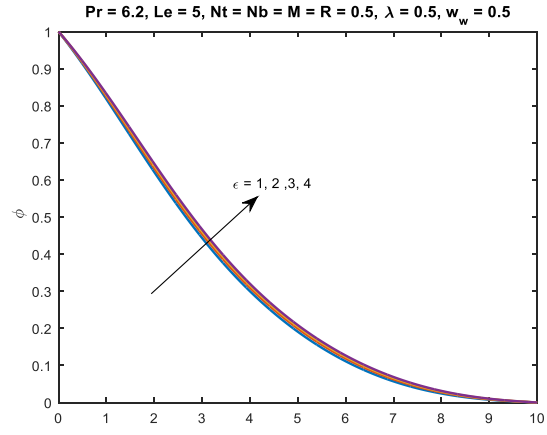

Fig. 5(b). Concentration profile for various values of ϵ .

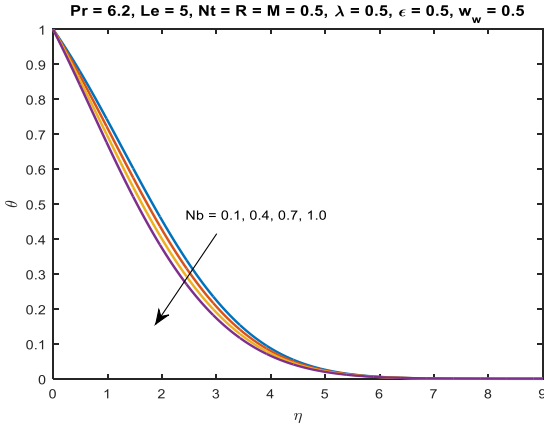

Fig. 6(a). Temperature profile for various values of Nb .

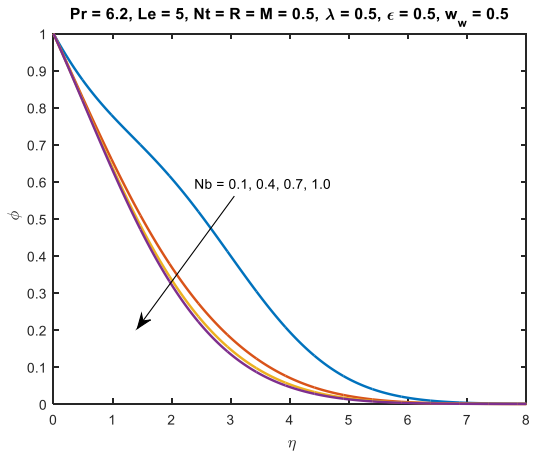

Fig. 6(b). Concentration profile for various values of Nb.

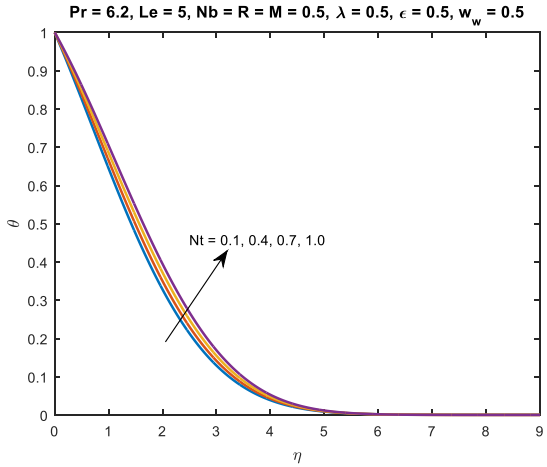

Fig. 7(a). Temperature profile for various values of Nt.

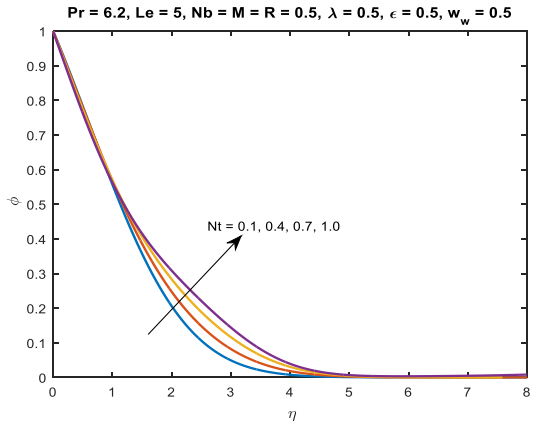

Fig. 7(b). Concentration profile for various values of Nt.

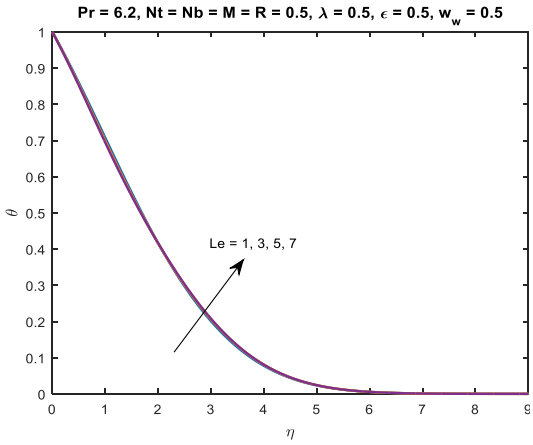

Fig. 8(a). Temperature profile for various values Le.

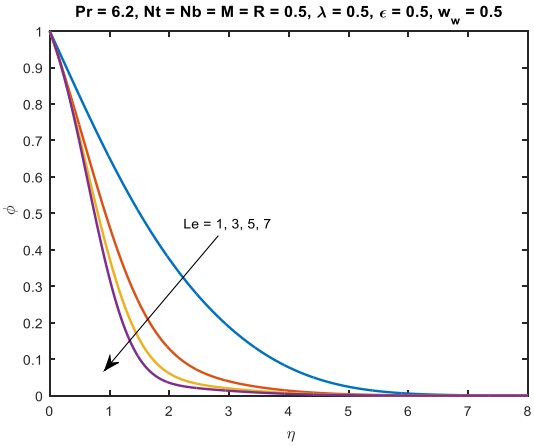

Fig. 8(b). Concentration profile for various values of Le.

From Fig. 6(b), it appears that the concentration profiles are squeezed for larger values of Brownian motion of parameter. The Brownian force tries to throw the particles in the opposite direction of the concentration gradient and make the nanofluid more homogenous. Hence the higher Brownian forces inherent in the lower concentration gradient.

Fig. 7(a) shows that the increasing values of thermophoresis parameter Nt lead to an upward trend in the temperature profile. Greater values in the thermophoresis parameter provide a stronger thermophoretic force which moves nanoparticles from

hotter place to cooler place areas and, as a consequence, the temperature profile and its related thickness of the thermal boundary layer are enhanced.

The effects of thermophoresis parameter Nt are observed on the concentration profile from Fig. 7(b). Here the concentration profiles are higher for the increasing values thermophoresis parameter. Intrinsically, the thermophoretic force tries to transfer the nanoparticles in the opposite direction of the temperature gradient, causing a non-uniform nanoparticles distribution. It is concluded that the more thermophoretic force, the more concentration gradient that indicates more non uniform concentration profiles.

Fig. 8(a) plotted the temperature profile for various values of Lewis number $Le.$ The number is used to describe the fluid flows that contain the process of momentum diffusion via Brownian diffusion. The Lewis number supports the enhanced temperature function.

Fig. 8(b) gives concentration profile for various values of Lewis number which reveals the concentration profile increases with Lewis number. Physically for larger values of the Lewis number, the Brownian diffusion effect is less important as compared to the momentum diffusion effect. Therefore, the effects of the Lewis number reduced the concentration boundary layer significantly.

Table 2 shows the heat transfer rate for various values of thermophoresis parameter, Brownian diffusion parameter and magnetic field parameter. From this table, we can observe that the heat transfer rate is lower when the values of thermophoresis parameter are larger. The Brownian diffusion parameter and magnetic field parameter are taken into account.

Table 1. Numerical values of $F(\eta)$, $G(\eta)$ and $-H(\eta)$ without heat and mass transfer and for $\lambda = M = w_w = \epsilon = 0$ and $R = 1$.

η	$F(\eta)$	$F(\eta)$	$G(\eta)$	$G(\eta)$	$-H(\eta)$	$-H(\eta)$
	Present work	**White [25]**	**Present work**	**White [25]**	**Present work**	**White [25]**
0.0	0.0000	0.0000	1.0000	1.0000	0.0000	0.0000
1.0	0.1802	0.1801	0.4768	0.4766	0.2654	0.2655
2.0	0.1187	0.1188	0.2033	0.2034	0.5725	0.5732
3.0	0.5657	0.0581	0.0824	0.0845	0.7439	0.7452
4.0	0.0254	0.0256	0.0344	0.0349	0.8227	0.8249
5.0	0.0104	0.0108	0.0137	0.0144	0.8559	0.8594

Table 2. Variations of local Nusselt Number for different values of Nt, Nb, M.

Nt	Nb	M	$-\theta'(0)$
0.1			0.2224
0.3	0.5	0.5	0.2153
0.5			0.2105
0.9			0.2073
	0.2		0.2369
0.5	0.4	0.5	0.2192
	0.6		0.2022
	0.8		0.1861
		0.1	0.2224
0.5	0.5	0.4	0.2127
		0.6	0.2088
		0.9	0.2051

8. Conclusion

A numerical study is carried out to investigate the flow of magneto-nanofluid over a porous rotating disk under the impact of slip, Brownian diffusion, and thermophoresis effects. The numerical experiments are conducted through the bvp4c technique. The major findings of the present study are outlined below:

- Larger values of magnetic parameter indicate the increasing behavior for temperature distribution and the same behavior is noticed for concentration distribution.
- For the values of unsteadiness parameter, the temperature profile as well as the concentration profile have been suppressed within the fluid flow.
- Increasing values of rotational parameter deplete the components of temperature and also the concentration distribution is depleted.
- The components of temperature and concentration are gone up for the increasing values of slip parameter.
- The temperature and concentration profiles are squeezed for the higher values of Brownian diffusion parameter.
- Temperature distribution and concentration distribution are higher for the values of thermophoresis parameter.
- The temperature function has experienced an ascending nature for increasing Lewis number while the concentration function is perceived the opposite nature.
- The heat transfer is lower when the larger values of thermophoresis parameter, Brownian diffusion and magnetic field are taken into account.

Acknowledgement

We would like to show our gratitude to the two anonymous reviewers for their scholarly insights. We are also immensely grateful to them for their comments on an earlier version of the manuscript, although any errors are our own and should not tarnish the reputations of these esteemed persons.

Nomenclature

B_0	Magnetic field strength
c_p	Specific heat at constant pressure
C	Nanoparticle volume fraction
C_w	Nanoparticle volume fraction at surface disk
C_∞	Ambient nanoparticle volume fraction
D_B	Brownian diffusion coefficient
D_T	Thermophoretic diffusion coefficient
F	Dimensional radial velocity
G	Dimensional tangential velocity
H	Dimensionless axial velocity
M	Magnetic field
k	Thermal conductivity
r	Cylindrical radial coordinate
Le	Lewis number
Nb	Brownian motion parameter
R	Rotational parameter
Nt	Thermophoresis parameter
Nu	Nusselt Number
p	Dimensional pressure
P	Dimensionless pressure
p_∞	Pressure of ambient fluid
Pr	Prandtl number
Re	Reynolds number
T	Temperature
T_w	Temperature at the surface of the disk
T_∞	Temperature of the ambient fluid
x, y, z	Dimensional coordinate
U_T	Target velocity
α	Thermal diffusivity
w_w	Suction and Injection velocity
ρ	Density
σ	Electric conductivity
θ	Dimensionless temperature
$(\rho c_p)_p$	Effective heat capacity of nanofluid
μ	Dynamic viscosity
λ	Unsteadiness parameter
η	Similarity Variable
φ	Cylindrical tangential coordinate
ϕ	Dimensionless concentration
Ω	Angular velocity
ϵ	Slip parameter
υ	Kinematic viscosity
ζ	Target momentum accommodation coefficient
δ	Time dependent length scale
λ^*	Mean free path
$(\rho c_p)_f$	Heat capacity of fluid

References

[1] Choi SUS. Enhancing thermal conductivity of fluids with nanoparticles. In: Siginer DA, Wang HP (eds.) Development and applications of non-Newtonian flows. ASME FED 1995; 231: 99-105.

[2] Masuda H, Ebata A, Teramae K, Hishinuma N. Alteration of thermal conductivity and viscosity of liquid by dispersing ultra-fine particles. Netsu Bussei 1993;7:227-233.

[3] Buongiorno J, Hu W, Nanofluid coolants for advanced nuclear power plants, Paper no. 5705, in: Proceedings of ICAPP'05, Seoul, and May 2005;15-19.

[4] Kakac S, Pramuanjaroenkij A. Review of convective heat transfer enhancement with nanofluids, Int. J. Heat Mass Transfer 2009;52:3187-3196.

[5] Wong KV, Leon OD. Applications of nanofluids: current and future. Adv Mech Eng. 2010;Article ID 519659 21.

[6] Saidur R, Leong KY, Mohammad HA. A review on applications and challenges of nanofluids. Renew Sustain Energy Rev (2011) 15:1646–1668.

[7] Wen D, Lin G, Vafaei S, Zhang K. Review of nanofluids for heat transfer applications. Particuology. 2011;7:141-150.

[8] Oztop HF., Abu-Nada E. Numerical study of natural convection in partially heated rectangular enclosures filled with nanofluids, Int. J. Heat Fluid Flow. 2008;29:1326-1336.

[9] Das SK, Choi SUS, Yu W. Pradeep T., Nanofluids: Science and Technology. Wiley Interscience, New Jersey, 2007.

[10] Buongiorno J. Convective transport in nanofluids. ASME J. Heat Trans. Vol. 2006;128: 240-250.

[11] Bachok N, Ishak A, Pop I, Flow and heat transfer over a rotating porous disk in a nanofluid. Phys B. 2011;406:1767-1772.

[12] Rajput GR, Krishnaprasad JSVR, Timol MG. Application of scaling group transformation for MHD boundary layer flow and heat transfer of nanofluids over moving surface subject to suction/injection in the presence of thermal radiation with chemical reaction, Int. J. Adv. Appl. Math. 2015;3(1):139-144.

[13] Von Ka´rma´n, Uber laminare und turbulentereibung. Z Angew Math Mech 1921;1:233-252.

[14] Nanda RS, Revolving flow of an incompressible fluid past a porous plate. J Sci Eng Res. 1960;5:59–64.

[15] Millsaps K, Pohlhausen K, Heat transfer by laminar flow from a rotating disk. J Aeronaut Sci. 1952;19:120-126.

[16] Batchelor GK, Note on the class of solutions of the Navier–Stokes equations representing steady non-rotationally symmetric flow, Q J Mech. Appl. Math. 1951;4:29-41.

[17] Owens JM, Rogers RH, Flow and heat transfer in rotating disk systems. Research Studies Press Ltd, Wiley, London, 1989.

[18] Attia HA, Unsteady MHD flow near a rotating porous disk with uniform suction or injection. Fluid Dyn Res. 1998;23:283–290.

[19] Bachok N, Ishak A, Pop I. Flow and heat transfer over a rotating porous disk in a nanofluid. Phys B., 2011;406:1767–1772.

[20] Turkyilmazoglu M, Senel P. Heat and mass transfer of the flow due to a rotating rough and porous disk. Int. J. Thermal Sci., 2013;63:146-158.

[21] Shafique Z, Mustafa M, Mushtaq A. Boundary layer flow of Maxwell fluid in rotating frame with binary chemical reaction and activation energy. Results Phys. 2016;6:627-633.

[22] Mushtaq A, Mustafa M, Hayat T, Alsaedi A. Numerical study for rotating flow of nanofluids caused by an exponentially stretching sheet. Adv Powder Technol. 2016;27:2223-2231.

[23] Ahmad R, Mustafa M. Model and comparative study for rotating flow of nanofluids due to convectively heated exponentially stretching sheet. J MolLiq 2016;220: 635–641.

[24] Hayat T, Muhammad T, Shehzad SA, Alsaedi A. On magnetohydrodynamic flow of nanofluid due to rotating disk with slip effect: A numerical study, Comput. Methods Appl. Mech. Engrg., 2017; 315: 467-477.

[25] White FM (1991). Viscous fluid flows, McGraw-Hill, Inc., New York.